Transcriptome Dynamics Reveal Stage-specific and Melatonin-triggered Gene Expression Patterns During the Cashmere Growth Cycle in Capra Hircus

Chun Li

Inner Mongolia University for Nationalities

Cong Feng

Zhejiang University College of Life Sciences

Guangyuan Ma

Zhejiang University College of Life Sciences

Shaoyin Fu

Inner Mongolia Academy of Agricultural and Animal Husbandry Sciences

Ming Chen (✉ mchen@zju.edu.cn)

Zhejiang University College of Life Sciences

Wenguang Zhang

Inner Mongolia Agricultural University

Jinquan Li

Inner Mongolia Agricultural University   https://orcid.org/0000-0002-8616-668X

RESEARCH

Transcriptome Dynamics Reveal Stage-specific and Melatonin-triggered Gene Expression Patterns during the Cashmere Growth Cycle in *Capra hircus*

Chun Li[1†], Cong Feng[2†], Guangyuan Ma[2†], Shaoyin Fu[3], Ming Chen[2,4*], Wenguang Zhang[5*] and Jinquan Li[5*]

*Correspondence:
mchen@zju.edu.cn;
atcgnmbi@yahoo.com.cn;
lijinquan_nd@126.com
[2]College of Life Sciences, Zhejiang University, Hangzhou 310058, China
[4]College of Life Science and Food Engineering, Inner Mongolia University for Nationalities, Tongliao 028000, China
[5]College of Animal Science, Inner Mongolia Agricultural University, Hohhot 010018, China
†These authors have contributed equally to this work.
Full list of author information is available at the end of the article

Abstract

Background: Cashmere goat is famous for its high-quality fibers. The growth of cashmere in secondary hair follicles exhibits a seasonal pattern arising from circannual changes in the natural photoperiod. Although several studies have compared and analyzed the differences in gene expression between different cashmere growth stages, the selection of samples in these studies relies on research experience or morphological evidence. Distinguishing cashmere growth cycles according to gene expression patterns may help to explore the regulation mechanisms related to cashmere growth and the effect of melatonin from a molecular level more accurately.

Results: In this study, we applied RNA-sequencing to the hair follicles of three normal and three melatonin-treated Inner Mongolian cashmere goats sampled every month during a whole cashmere growth cycle. A total of 3559 and 988 genes were subjected as seasonal changing genes (SCGs) in the control and treated groups, respectively. The SCGs in the normal group are divided into three clusters, and their specific expression patterns help to group the cashmere growth cycle into anagen, catagen and telogen stages. Some canonical pathways such as Wnt, TGF-beta and Hippo signaling pathways are detected as promoting the cashmere growth, while Cell adhesion molecules (CAMs), Cytokine-cytokine receptor interaction, Jak-STAT, Fc epsilon RI, NOD-like receptor, Rap1, PI3K-Akt, cAMP, NF-kappa B and many immune-related pathways are detected in the catagen and telogen stages. The PI3K-Akt signaling, ECM-receptor interaction and Focal adhesion are found in the transition stage between telogen to anagen, which may serve as candidate biomarkers for telogen-anagen regeneration. Pairwise comparisons between the control and melatonin-treated groups also indicate 941 monthly differentially expressed genes (monthly DEGs). These monthly DEGs are mainly distributed from April and September, which reveal a potential signal pathway map regulating the anagen stage triggered by melatonin. Enrichment analysis shows that Wnt, Hedgehog, ECM, Chemokines and NF-kappa B signaling pathways may be involved in the regulation of non-quiescence and secondary shedding under the influence of melatonin.

Conclusions: Our study decodes the key regulators of the whole cashmere growth cycle, laying the foundation for the control of cashmere growth and improvement of cashmere yield.

Keywords: cashmere growth cycle; hair follicle; RNA-seq; melatonin; signaling pathway

1 Background

2 The Inner Mongolian cashmere goat (*Capra hircus*), an excellent cashmere goat breed

3 in China, is famous for producing cashmere with superior quality and high yield. Inner

4 Mongolian cashmere goats have two distinctly different fibrous hair structures, with

5 thick, coarse guard hairs forming the outer layer and fine, soft ground hairs forming the

6 cashmere underneath. The cashmere comes from secondary hair follicles (SHFs) in the

7 skin [1], and the coarse hair comes from primary hair follicles [2, 3]. The cashmere

8 obtained from goats is used exclusively in the production of luxurious textile products

9 [4]. The growth of cashmere in the Inner Mongolian cashmere goat exhibits a seasonal

10 pattern arising from circannual changes in the natural photoperiod. The cashmere

11 growth cycle typically starts in July and stopping the following March with shedding

12 of the fleece at the end of April [5].

13 Melatonin is a critical intermediary between photoperiod and cashmere growth, and

14 circulating melatonin levels directly affect cashmere growth [6]. Previous studies have

15 shown that the use of exogenous melatonin could stimulate cashmere growth during the

16 resting period. However, the implanting time and duration of melatonin could result in

17 earlier cashmere shedding followed by another typical cycle of cashmere growth [6-9],

18 or increase cashmere yield by combining the induced growth of cashmere fleece [10,

19 11]. It has been confirmed that exogenous melatonin has a positive role on cashmere

20 growth. Unfortunately, previous experiments have not been able to show the cashmere

21   growth cycle related gene expression profiles and the potential roles of exogenous

22   melatonin on cashmere growth.

23   Hair follicle growth in the skin of cashmere goats changes dynamically after birth and

24   continues in a cyclical pattern. The cashmere growth cycle can be divided into three

25   phases: telogen, anagen, and catagen, each of which is regulated by specific genetic

26   patterns [5]. With the rapid development of high-throughput sequencing technology,

27   some regulatory factors and signaling pathways involved in the hair follicle cycle have

28   been found through differential expression and functional enrichment analysis. These

29   well-known regulatory molecules and signaling pathways include Wnt/β- catenin [12-

30   14], bone morphogenetic proteins (BMPs) [15, 16], sonic hedgehog (SHH) [17], notch

31   [18], fibroblast growth factors (FGFs) [19], transforming growth factors (TGFs) [20]

32   and keratin-associated proteins (KRTAPs) [5, 21], etc.

33   Long noncoding RNAs (lncRNAs) are RNAs that are longer than 200 nucleotides but

34   do not encode proteins. However, lncRNAs can regulate the expression of protein-

35   coding genes at various levels, including epigenetic regulation, transcriptional

36   regulation and posttranscriptional regulation, thereby influencing various biological

37   processes. Recent studies have reported the mechanisms of lncRNAs in hair growth and

38   development in cashmere goats. For example, several important hair follicle

39   development signals (lncRNAs and mRNAs) are involved in primary wool follicle

40   induction in carpet sheep [22]. Yin et al. indicated that lncRNA-599554 contributes the

41   inductive property of dermal papilla cells in cashmere goat, which might be achieved

42   through sponging chi-miR-15b-5p to promote the WNT3A expression [23]. Wang et al.

43   integrated analysis of lncRNA, miRNA and mRNA in cashmere goat skin during

44   anagen and telogen stages and revealed potential ceRNA regulatory networks [24, 25].

45   Sulayman et al. performed a comprehensive analysis of lncRNA and mRNA expression

46   profiles during sheep fetal and postnatal hair follicle development and demonstrated

47   that the interaction between lncRNA and their target genes may regulate the

48   development of hair follicles [26]. However, the roles of lncRNAs in controlling the

49   whole cashmere growth cycle have not been well described.

50   To clarify the regulatory mechanism of cashmere growth cycles and gain insight into

51   the gene regulatory network perturbed by exogenous melatonin, we use RNA-seq

52   analysis to investigate the expression patterns of seasonal changing genes (SCGs)

53   among different gene clusters. The interactions between lncRNAs and mRNAs were

54   also explored using co-expression network analysis. The monthly differentially

55   expressed genes obtained from pairwise comparisons between the control and

56   melatonin-treated groups were detected to identify the key regulators associated with

57   the growth of secondary hair follicles and reveal potential signaling pathways which

58   may be involved in melatonin-affected growth patterns.

59

60

61

62

63

Methods

Skin sample and cashmere collection

We enrolled six cashmere goats of the same gender and age. All goats were randomly divided into two groups: control group (D) and melatonin group (M). Three cashmere goats in the experimental group were subcutaneously implanted with melatonin for one year since December 2014. The control group was untreated. The skin samples from the six cashmere goats were collected monthly (Jan 19th, Feb 13th, Mar 21st, Apr 18th, May 20th, Jun 20th, Jul 18th, Aug 23rd, Sept 19th, Oct 20th, Nov 20th, and Dec 20th) from both the control and melatonin groups. Immediately after collection, all samples were frozen in liquid nitrogen and stored at $-80°C$ until use. At each sampling time point, 50 cashmeres were taken from each goat to measure the cashmere length.

RNA extraction, library preparation and sequencing

Total RNA from 72 collected skin samples were isolated using the TRIzol[TM] reagent (Invitrogen, USA) following the manufacturer's instructions. RNA degradation and contamination was monitored on 1% agarose gels. RNA purity was verified using the NanoPhotometer® spectrophotometer (Implen, USA). RNA integrity was checked using the RNA Nano 6000 Assay Kit (Agilent Technologies, USA). For the RNA library preparation, ribosomal RNA (rRNA) was removed first by the Epicentre Ribo-zero[TM] rRNA Removal Kit (Epicentre, USA) from 3 μg total RNA. Then, sequencing libraries were generated using the NEBNext® Ultra[TM] Directional RNA Library Prep Kit for Illumina (NEB, USA) following manufacturer's instructions. Finally, the strand-specific libraries were sequenced on the Illumina Hiseq 4000 system (paired-end 150

86   bp reads).

Quality control

88   FastQC [27] is used to filter out low-quality residues and joints of raw reads produced

89   by RNA-seq. The quality of clean reads (Q20, Q30, and GC content) were detected.

90   The high quality clean reads are retained for subsequent analysis.

Read alignment and transcriptome assembly

92   Clean reads were aligned to the goat genome (NCBI assembly ARS1) using HISAT2

93   [28] under default settings. The mapped reads of each sample were assembled by

94   StringTie [28] in a reference-based mode. All transcripts assembled were merged into

95   a Gene transfer format (GTF) file.

Novel lncRNA identification

97   The transcripts without matching the known annotations were selected to identify novel

98   lncRNAs through the following steps: (1) transcripts less than 200 bp in length were

99   removed; (2) transcripts with exon number less than 2 were removed; (3) the coding

100   potential of each transcript was predicted using CPC2 [29] and CNCI [30], and

101   transcripts predicted as "noncoding" were imported into Pfam Scan

102   (http://ftp.ebi.ac.uk/pub/databases/Pfam/Tools/) to filter out those with known protein

103   family domains (Pfam release 30).

Reads counting and time-series differential expression analysis

105   All coding genes and lncRNA genes were included to calculate the count matrix using

106   htseq-count [31]. The likelihood ratio test (LRT) in DESeq2 [32] was used to identify

107   the seasonal changing genes (SCGs) in both control and melatonin group with model

108 "~ time" versus "~ 1". Here SCGs are defined as genes with significant expression

109 changes throughout the cashmere growth cycle. Initially, the count matrix was

110 normalized by the size factors estimated by DESeq2 and the median of the normalized

111 gene expression values at each time point were used to calculate the fold change f_i:

112 $$\mu_{it} = median_j \left(G_{ijt} \right)$$

113 $$f_i = \frac{max_t \left(\mu_{it} \right)}{min_t \left(\mu_{it} \right) + 1}$$

114 Where G_{ijt} is the normalized expression value of gene i in goat j at sampling time t.

115 The thresholds for adjusted p-value and fold change were set to 0.05 and 2, respectively.

116 Besides, the differential changing genes (DCGs) between control and melatonin group

117 were detected using LRT with model "~ time + condition + time: condition" versus "~

118 time + condition".

Gene cluster detection

120 The SCGs detected in control group were included for weighted gene co-expression

121 network analysis (WGCNA) [33]. Pearson correlations between gene clusters and trait

122 data (months) were calculated. The minimum cluster size was set to 50, and clusters

123 with a tree height less than 0.25 in the dendrogram were merged.

Pathway enrichment

125 The DAVID database [34] was used to identify the significantly enriched Kyoto

126 Encyclopedia of Genes and Genomes (KEGG) pathways [35] for gene modules

127 detected by WGCNA. The p-value threshold for enrichment was set to 0.05. The

128 pathways enriched in infectious diseases and cancer were removed.

129 Monthly DEGs were annotated with Gene Ontology (GO) [36] biological process (BP)

130   and KEGG analysis. The annotations were all achieved with clusterProfiler [37]

131   package, with q-value ≤ 0.05 for GO and p-value ≤ 0.05 for KEGG. Annotation

132   information was retrieved from the Ensembl database using AnnotationHub [38] to

133   generate an OrgDb annotation file.

134   **Pathway-mRNA-lncRNA network construction**

135   We selected genes enriched in key signaling pathways as sources, and co-expressed

136   lncRNA genes as targets to construct the pathway-mRNA-lncRNA network. The

137   Pearson correlations between pathway genes and lncRNA genes were calculated, and

138   those mRNA-lncRNA pairs with correlation higher than 0.8 were selected to construct

139   the network. CytoScape [39] was used to visualize the network.

140   **Calculation of relative gene expression for monthly DEGs**

141   To observe the effects of melatonin on the expression of representative differentially

142   expressed gene, we plotted relative expression boxplots to visually compare the

143   expression trends of these genes. The horizontal axis of the boxplot represents months,

144   and the vertical axis represents relative expression levels, which were calculated as

145   follows:

146   $$relative\ expression\ level = \ln\left(\frac{Gene\ Counts\ in\ Melatonin}{Gene\ Counts\ in\ Control}\right)$$

147   The gene counts were normalized with total counts in different groups. Three relative

148   expression values per month were used for boxplot visualization.

149

150

151

Results

Transcriptome analysis and differential gene expression overview

A total of 72 samples spanning 12 months were analyzed in the control (D) and melatonin (M) groups (**Figure 1A**). The experiments produced 2,959,842,480 clean reads in total (~926G). A total of 22,404 genes were detected from reads counting through the RNA-seq data analysis (**Additional file 1: Table S1**). A total of 2365 novel lncRNA genes were identified after the protein-coding-potential test (**Additional file 2: Table S2**). Using DESeq2 time-series data analysis, 3559 and 988 genes were subjected as SCGs by fold change ≥2 and adjusted p-value ≤0.05 in the D and M groups, respectively (**Figure 1B**) (**Additional file 3: Table S3 and Additional file 4: Table S4**). Among these SCGs, a total of 345 novel lncRNAs and 211 annotated lncRNAs were detected in the D group. We found that SCGs in the M group were much less than those in the D group, and 76.8% (759) of the SCGs in the M group also existed in the D group (Figure 1C). According to the PCA diagrams in **Figures 1D** and **1E**, the samples of the D group showed a certain periodic distribution, but the sample distribution was disturbed after the melatonin treatment. It can be seen in **Figure 1F** and **1G** that the goats in two groups shed the cashmere in May, while goats in the M group had another shedding in September-November. An interesting finding is that in the M group, new cashmere has grown during the shedding in May, that is, the SHFs have not entered the resting period and the cashmere growth cycle has restarted in advance (**Figure 1G**).

Stage-specific gene expression dynamics in the cashmere growth cycle

The correct division of the cashmere growth cycle is the basis for subsequent

identification and analysis of regulatory factors. The existing studies are mostly based

on morphological evidence or prior knowledge. A recent study divided the cashmere

growth cycle into growth period, regression period and resting period based on skin

tissue sections and transcriptome data [5]. However, their analysis is based on static

differential expression analysis, the dynamic change of gene expression has not been

well studied. In our study, we analyzed the time-series transcriptome data covering the

entire cashmere growth cycle and obtained 3559 SCGs. Through WGCNA analysis,

three key gene clusters (DC1, DC2 and DC3) that may be involved in the growth cycle

of villi were identified in the D group (**Figure 2A**)*.* The detailed genes of three clusters

are listed in **Additional file 5: Table S5**, which encompass 48.2% (1717) of the SCGs

detected in the D group, including 91 annotated lncRNAs and 131 novel lncRNAs

(**Figure 2B**). Combining the expression patterns and functional enrichment results of

three clusters (**Figure 2A** and **2C**), we inferred the effects of these clustered genes on

the cashmere growth cycle. The genes in DC1 may promote cashmere growth and the

genes in DC2 may be related to the regression of the SHFs. There may be an

antagonistic relationship between DC1 and DC2, which can also be inferred from the

gene expression trends in **Figure 2D**. The gene expression in DC1 began to be up-

regulated in April and reached a peak in October and started to be down-regulated,

while the gene expression pattern in DC2 was exactly the opposite. In addition, it can

also be found that the high expression of DC3 occurs when the expression of DC1 genes

195   begins to be up-regulated and the expression of DC2 genes begins to down-regulate.

196   Based on the above analysis, we divided the cashmere growth cycle into three stages

197   associated with three gene clusters: (1) anagen (April-October); (2) catagen and telogen

198   (October-December and January-April); (3) telogen-anagen regeneration (February-

199   May). The detailed functional analysis of these three clusters and their relationships

200   with the cashmere growth cycle are discussed below.

201   **The DC1 cluster shows high expression in anagen progression stage**

202   A total of 394 genes in DC1 (including 22 annotated lncRNAs and 52 novel lncRNAs)

203   are positively correlated with the anagen progression stage (April-October), which may

204   be involved in promoting the cashmere growth (**Figure 2A and Figure 2D**). Some

205   canonical pathways such as the Wnt, TGF-beta and Hippo signaling pathways, which

206   have been proven to be closely related to hair growth [14, 40, 41] are also enriched in

207   DC1 (**Figure 2C**) (**Additional file 6: Table S6**). Three genes of the Wnt family

208   WNT2/WNT2B/WNT11, together with their receptors FZD3 and FZD10 are involved

209   in the regulation of the SHF development in cashmere goats. Lymphoid enhancer

210   binding factor-1 (LEF1) is an essential transcription factor in the Wnt signaling, and it

211   was strongly expressed during the anagen progression stage in this study. Its function

212   in hair cell differentiation and follicle morphogenesis has already been discussed [42].

213   Genes in the TGF-beta signaling (BMP2, BMP8A, BAMBI and SMAD6) also showed

214   similar patterns with the Wnt family. It is found that the genes enriched in the Hippo

215   signaling overlap with those in the Wnt and TGF-beta signaling, indicating the crosstalk

216   between Wnt and TGF-beta signaling formed by the joint regulation of downstream

217   pathways [14, 43]. In addition, some downstream regulatory mechanisms of hair

218   growth and cycling were also confirmed in this study. For example, the homeobox

219   transcription factor DLX3 and one of its regulating genes, HOXC13, were also highly

220   expressed in the anagen stage. The regulatory cascade positions DLX3 downstream of

221   Wnt signaling and regulates other transcription factors related to hair follicle (HF)

222   differentiation (such as HOXC13) [44]. KRTs (KRT26, KRT35, KRT36, KRT39,

223   KRT6A, KRT74 and KRT84) and KRTAPs (KRTAP3-1 and KRTAP11-1) in DC1

224   were also associated with HF development [45]. SHH and its receptor PTCH2 in the

225   sonic hedgehog (Shh) signaling pathway were also found in DC1. The function of Shh

226   signaling is indicated as an essential regulator for controlling ingrowth and

227   morphogenesis of the HFs [46-48], but it is not necessary for initiating the HF

228   development [46].

229   **The DC2 cluster prefers to be highly expressed in catagen and telogen**

230   A total of 919 genes in DC2 (including 45 annotated lncRNAs and 53 novel lncRNAs)

231   were up-regulated from October to April of the following year (**Figure 2A and 2D**),

232   which corresponded to the degenerative and resting periods of the cashmere growth

233   cycle. It should be pointed out that due to the limitation of sampling interval, the catagen

234   and telogen stages were not further distinguished in this study. The expression pattern

235   of DC2 is negatively correlated with DC1, suggesting that there may be an antagonistic

236   relationship between the genes in DC2 and DC1. DC2 genes are mainly enriched in

237   pathways such as Cell adhesion molecules (CAMs), Cytokine-cytokine receptor

238   interaction, Jak-STAT, Fc epsilon RI, NOD-like receptor, Rap1, PI3K-Akt, cAMP, NF-

239   kappa B and many immune-related pathways (**Figure 2C**) (**Additional file 6: Table**

240   **S6**). A previous study also found that differentially expressed genes between anagen

241   and telogen SHF-derived dermal papilla cells of the Cashmere goat were also enriched

242   in CAMs and Cytokine-cytokine receptor interaction pathways [49]. A number of

243   interleukin (IL) superfamily genes were involved in the enriched pathways of DC2,

244   such as the IL1 family (IL7 and IL18), IL10, IL15, and IL receptors (IL2RG, IL3RA,

245   IL6R, IL7R, IL11RA and IL20RA). The CC chemokine subfamily (CCL5, CCL21,

246   CCL22 and CCL26) and receptors (CCR4 and CCR6) were also found in the DC2

247   cluster. These chemokines are mainly involved in cell migration, immunity and

248   inflammation [50]. During the HF regression, these chemokines may guide the

249   migration of immune cells such as dendritic cells [51] and Regulatory T cells [52],

250   thereby regulating the immune response to apoptotic cells. The JAK3 and STAT4 genes

251   in the JAK-STAT signaling were highly expressed in catagen and telogen, which have

252   been found to maintain HF stem cell quiescence and inhibit hair growth [53-55]. In

253   addition, Dickkopf1 (DKK1), a Wnt signaling inhibitor, was also found in DC2. DKK1

254   has been strongly suggested to promote regression of HFs by suppressing Wnt/β-

255   catenin signaling and inducing apoptosis in follicular keratinocytes [56, 57].

256   **The DC3 cluster is specifically expressed in telogen-anagen regeneration stage**

257   DC3 cluster contains a total of 404 genes (including 24 annotated lncRNAs and 26

258   novel lncRNAs) and shows specific high expression during the transition period from

259   February to May (**Figure 2A and 2D**). Due to the overlap of the early anagen and

260   telogen-anagen regeneration stages, the genes of DC3 and DC2 were partially enriched

261 in several same pathways like CAMs, Focal adhesion, extracellular matrix (ECM)-

262 receptor interaction, PI3K-Akt and NF-kappa B signaling (**Figure 2C**) (**Additional file**

263 **6: Table S6**). The PI3K-Akt signaling has been proved to be essential for HF

264 regeneration [58, 59]. A previous study found that the Toll-Like Receptor 3 (TLR3)

265 activated by a dsRNA was able to promote HF regeneration [60]. Several collagen

266 genes (COL1A1, COL1A2, COL3A1, COL5A2, COL6A3, COL6A5 and COL6A6) in

267 the PI3K-Akt signaling, ECM-receptor interaction and Focal adhesion were found in

268 DC3. These collagen genes may serve as candidate biomarkers for telogen-anagen

269 regeneration. For example, a kind of self-assembling peptide hydrogel scaffold was

270 used to build the ECM environment in vitro to promote HF regeneration [61].

271 **Pathway crosstalk through mRNA-lncRNA co-expression network in**

272 **cashmere growth cycle**

273 A total of 16 signaling pathways, 145 pathway genes, and 93 co-expressed lncRNAs

274 (Pearson correlation ≥0.8) (**Additional file 7: Table S7**) are enrolled in this pathway-

275 mRNA-lncRNA network (**Figure 3**). It can be seen that the DC1 sub-network has no

276 positive correlation with DC2 and DC3, which can be explained by the possible

277 antagonistic relationship between DC1 and DC2. The telogen-anagen transition phase

278 of DC3 overlaps with the telogen stage, so the DC3 subnet is closely connected to DC2.

279 Through this network, the function of lncRNAs can be inferred by their co-expressed

280 coding genes. Three novel lncRNAs (LNC.6206, LNC.8064 and LNC.16941) are

281 highly connected (by more than 6 coding genes) in the DC1 sub-network, indicating

282 that they may mediate in promoting HF development. Similarly, four novel lncRNAs

283 (LNC.348, LNC.6138, LNC.11657 and LNC.14789) and two annotated lncRNAs

284 (LOC106503915 and LOC108637283) were found with high degrees in the DC2 sub-

285 network. The coding genes connected to them cover all the signaling pathways in DC2,

286 indicating that these lncRNAs are likely to be involved in the SHF degeneration. The

287 PI3K-Akt and NF-kappa B signaling are both functioning in DC2 and DC3 sub-

288 networks. 9 novel lncRNAs and 4 annotated lncRNAs connecting DC2 and DC3 may

289 play a role in the transition from telogen to early anagen.

290 **Expression differences triggered by melatonin reveal a potential signal**

291 **pathway map regulating cashmere growth**

292 A total of 908 genes were detected to have different expression patterns between the D

293 group and the M group (**Figure 4A**) (**Additional file 8: Table S8**). When treated with

294 melatonin, 80 (24.6%) genes in DC3 maintained the same pattern as group D, but the

295 expression patterns of most genes in DC1 and DC2 have changed (**Figure 4B**). Among

296 the 908 differential changing genes (DCGs), 369 genes belonging to the three clusters

297 DC1, DC2 and DC3 were divided into three clusters MC1 (159), MC2 (144) and MC3

298 (66), respectively (**Figure 4C**) (**Additional file 9: Table S9**). After melatonin treatment,

299 MC1 and MC2 in the M group lost the periodic expression fluctuations as in the D

300 group (**Figure 4D**). In Apr-May, gene expression of MC1 dropped to the lowest while

301 expression of MC2 rose to the highest in the D group and shedding appeared. Pathway

302 enrichment showed that MC1 and MC2 were involved in the promotion and regression

303 of HFs, respectively (**Figure 4E**) (**Additional file 10: Table S10**). In the M group, the

304 expression of MC1 was still rising and MC2 was falling from January to April, which

305   may lead to a non-resting period after shedding in the M group. Therefore, genes in

306   MC3, which may be responsible for restarting HF growth, did not show a significant

307   increase in expression in February-May. In September-November, the expression of

308   MC1 in the M group was relatively lower than that in the D group, while the expression

309   of MC2 in the M group was higher than that in the D group, which may disrupt the

310   growth and maintenance of HFs and cause a local shedding.

311   To reveal the differential expression pattern every month, we use DESeq2 to obtain

312   monthly differentially expressed genes (monthly DEGs) between melatonin and control

313   groups with adjusted p-value (padj) ≤0.05 and |log2FoldChange| ≥1. A total of 941

314   monthly DEGs were identified from monthly pairwise comparisons. The monthly

315   DEGs are mainly distributed from April and September (**Figure 5A**), which exactly

316   cover the whole anagen stage, and 96% of them are protein-coding genes. The KEGG

317   analysis results (**Figure 5B**) (**Additional file 11: Table S11**) showed that Hedgehog

318   related genes (SHH, PTCH2, PTCH1) and Wnt related genes (FZD10, WIF1, LEF1,

319   WNT11) were up-regulated in April, while the GO results (**Figure 5C**) (**Additional**

320   **file 12: Table S12**) showed that Hedgehog genes (PTCH2, FOXE1) and other related

321   up-regulated genes like FOXN1, HOXC13, KRT25 and KRT71 were significantly

322   enriched from April to May. Related studies have shown that Wnt [62-64] and Shh [46,

323   65] signaling can promote hair follicle cell division and the initiation of anagen; C.

324   Potter et al. demonstrated that nude mutant gene FOXN1 is a regulatory target of

325   HOXC13 and the knockdown of both genes could cause abnormal hair growth [66]. Yu

326   et al. showed that a missense mutation at the helix terminus of KRT25 can cause a

327   reduction of woolly hair [67]. KRT71 is an inner root sheath keratin, and the mutant of

328   KRT71 can disrupt keratin intermediate filament formation [68]. Therefore, the

329   Hedgehog related genes (SHH, PTCH2, PTCH1, FOXE1), Wnt related genes (FZD10,

330   WIF1, LEF1, WNT11), and other hair development related genes FOXN1, HOXC13,

331   KRT25 and KRT71 may be responsible for the initiation of a fast anagen progressing

332   stage from April to July. Meanwhile, the KEGG results (**Figure 5B**) showed that the

333   expression of ECM receptor interaction genes (COL6A3, THBS3, COL1A1, FRAS1,

334   FREM1/2) was downregulated from June to July. ECM is an important matrix required

335   for hair follicle cell growth. Xu et al. showed that the amount of ECM occupied by each

336   cell determined the volume size of dermal papilla (DP) in hair follicles [69], and Zhu

337   et al. demonstrated that the rapid growth of anagen hair follicles in cashmere goat

338   required high expression of ECM and cell surface proteins [1]. The down-regulation of

339   ECM-related genes from June to July may contribute to the inhibition of hair follicle

340   growth, and the down-regulation of genes involved in the Hedgehog (SHH, PTCH2)

341   and Wnt (WNT6, NOTUM, SFRP2) pathways indicated that hair follicle growth may

342   be inhibited in August. The expression of genes in chemokine signaling pathway

343   (CCL17, CCL22, CCL2, LYN, RAC2, LOC102170772, PIK3CG, VAV1) was up-

344   regulated in September. Experiments by Nagao et al. have shown that chemokines can

345   induce immune cell migration as the hair follicle enters the catagen phase [51], which

346   may further promote the hair follicle apoptosis. Therefore, the downregulated ECM

347   receptor interaction genes (COL6A3, THBS3, COL1A1, FRAS1, FREM1, FREM2),

348   Hedgehog genes (SHH, PTCH2), Wnt genes (WNT6, NOTUM, SFRP2) and up-

349   regulated chemokines (CCL17, CCL22, CCL2, LYN, RAC2, LOC102170772,

350   PIK3CG, VAV1) may contribute to the second cashmere shedding happened from

351   August to November. Jin et al.'s transcriptome analysis of the melatonin-treated group

352   with MTC knockdown experiments confirmed that melatonin can promote hair follicle

353   development by activating the NF-kappa B pathway through promoting the expression

354   of MTC [70]. Genes in NF-kappa B signaling pathway (CD40LG, LTB,

355   LOC102176695, LYN, BTK) were up-regulated in September, which may contribute

356   to the hair follicle development after the second cashmere shedding. The representative

357   GO & KEGG enrichment results of monthly DEGs mentioned above were summarized

358   in **Table 1**.

359   Discussion

360   In this study, the cashmere goat skin samples of the experimental group and the control

361   group covered 12 months, that is, the entire cashmere growth cycle. Many studies have

362   used RNA-seq to explore the differences in gene expression in different growth stages

363   of cashmere. For example, Geng et al. conducted a functional analysis of the differences

364   in gene expression between three developmental stages of hair follicles in cashmere

365   goats, and identified key genes that are involved in the regulation of cashmere growth

366   [71]. Zhang et al. performed transcriptome sequencing analysis on hair follicles in four

367   seasons and explored the regulation of seasonal variation genes on the cashmere growth

368   cycle of the cashmere goat and milk goat [72]. However, these studies only selected

369   three or more stages determined by experiments or experience at the cellular level.

370   There is still a lack of research on the in-depth exploration of the dynamic pattern of

371   gene expression during different cashmere growth stages on the scale of whole cycles.

372   Therefore, this study performed transcriptome sequencing on the skin samples covering

373   the entire cashmere cycles for 12 months, which aims to explore the dynamics of gene

374   expression in the cashmere growth cycle in more detail.

375   The gene expression pattern for 12 months can provide useful information for

376   distinguishing different cashmere growth stages from the genetic and molecular levels.

377   According to the cluster-month correlations in Figure 2C, we grouped the cashmere

378   growth cycle into three main stages: (1) anagen (April-October); (2) catagen and

379   telogen (October-December and January-April); (3) telogen-anagen regeneration

380   (February-May). The corresponding gene clusters are DC1, DC2 and DC3, respectively.

381   Some canonical pathways such as the Wnt, TGF-beta and Hippo signaling pathways

382   are enriched in DC1. DC2 genes are mainly enriched in pathways such as Cell adhesion

383   molecules (CAMs), Cytokine-cytokine receptor interaction, Jak-STAT, Fc epsilon RI,

384   NOD-like receptor, Rap1, PI3K-Akt, cAMP, NF-kappa B and many immune-related

385   pathways. Interestingly, due to the overlap of the early anagen and telogen-anagen

386   regeneration stages, the genes of DC3 and DC2 were partially enriched in several same

387   pathways like CAMs, Focal adhesion, extracellular matrix (ECM)-receptor interaction,

388   PI3K-Akt and NF-kappa B signaling. Besides, by constructing a co-expression network

389   of genes (that are enriched in key pathways) and lncRNAs in three clusters, we reveal

390   the possible regulators for crosstalk between different signaling pathways, and

391   unearthed novel lncRNAs that may participate in these pathways.

392   In addition to unraveling the gene expression regulation mechanisms of the transition

393   between different stages of the hair follicle cycle, this study also helps to figure out the

394   role of exogenous melatonin in the specific stages of the cashmere growth cycle. By

395   identifying genes that exhibit different expression patterns during the cashmere growth

396   cycle under the stimulation of melatonin, we also obtained three gene clusters (MC1,

397   MC2 and MC3) that may affect the cashmere growth cycle. Among them, MC1 genes

398   (BAMBI, BMP2, BMP8A, FZD10, LEF1, PPP2R1B, SMAD6 and WNT11) and MC2

399   genes (IL6R, IL7R, IL11RA, IL15, IL18, PDE1A, PDE1B and PDE3B) showed

400   opposite periodicity in group D. However, after the melatonin treatment, this regular

401   fluctuation has been disordered. MC3 genes (COL1A1, COL1A2, COL3A1, CHAD,

402   CREB3L1 and THBS3) were expressed specifically in the anagen restart phase (Apr-

403   May) in group D, but there was no similarly significant expression pattern in group M.

404   The relative expression levels of monthly DEGs (**Additional file 13**) show that the hair

405   development related genes HOXC13, KRT25, KRT71, FOXN1 were generally

406   expressed at higher levels at the beginning of fast anagen progressing period from April

407   to May, implying that they may function to promote the initiation of anagen. Wnt genes

408   (Wif-1, WNT11, FZD10, LEF1, NOTUM, SFRP2, WNT6) together with Hedgehog

409   genes (SHH, PTCH1, PTCH2, FOXE1) showed higher expression levels between April

410   and May, but decreased in August, which implied that Wnt-related genes may promote

411   the rapid transition into anagen phase of hair follicles between April and May, and

412   repress the growth of hair follicles on the eve of the second cashmere shedding period

413   in August. Chemokines (CCL17, CCL22, CCL2, LYN, RAC2, LOC102170772,

414   PIK3CG and VAV1) and NF-κB genes (ZAP70, LYN, BTK, CD40LG, LTB) were

415   highly expressed in September. The NF-κB pathway may facilitate the progress of the

416   subsequent cashmere growth phase. Meanwhile, chemokines such as LTN may

417   promote the second cashmere shedding.

418   KEGG pathway could be used as a reference to demonstrate the regulatory relationships

419   of differentially expressed genes. Taking the above results together and collating the

420   relevant KEGG pathway visualization results (**Additional file 14**), here we proposed a

421   signaling pathway diagram of melatonin influenced cashmere growth cycle (**Figure 6**),

422   which covered the main differentially expressed genes related to cashmere growth in

423   anagen phase from April to September. The anagen phase of melatonin-treated groups

424   was composed of a fast anagen progressing stage and a second cashmere shedding stage.

425   The fast anagen progressing stage was from April to July, and this period was

426   characterized by the occurrence of the first massive cashmere shedding at the end of

427   April, and the rapid transition into anagen phase of hair follicles from May to July,

428   when the quick resumption of cashmere growth appeared instead of residing in a resting

429   non-growth period. The rapid resumption of the anagen phase of hair follicles may be

430   due to the high expression of KRT25, HOXC13 and HOXC13's regulatory target

431   FOXN1, high expression of FZD10, WIF1, LEF1, WNT11 in Wnt signaling pathway,

432   and SHH, PTCH1, PTCH2, FOXE1 in sonic hedgehog signaling pathway. The second

433   cashmere shedding period was from August to September. The appearance of the

434   second cashmere shedding may not only be associated with the low expression of ECM

435   signaling molecules such as FREM1, FREM2, FRAS1, COL1A1, COL6A3, THBS3 in

436   June and July, sonic hedgehog signaling pathway genes such as SHH, PTCH2 and

437   WNT signaling pathway genes such as NOTUM, SFRP2, WNT6 in August, but also

438   with the high expression of chemokines such as CCL, LYN, PIK3CG, VAV1, RAC2

439   in August. In addition, the highly expressed genes in NF-kappa B signaling pathway

440   such as CD40LG, LTB, ZAP, LYN, BTK in September may promote the subsequent

441   growth of cashmere after the second cashmere shedding period.

Conclusions

443   In summary, this study systematically analyzed RNA-seq data from skin samples of

444   cashmere goats covering the entire cashmere growth cycle and identified a series of key

445   regulators (including genes and lncRNAs) that may be involved in the cashmere growth

446   processes. Based on gene expression patterns, we elucidated a more precise division of

447   the cashmere growth cycle from the molecular level. However, due to the lack of

448   sampling points, some key stages (especially the transition state) are still not well

449   identified. A possible way is to increase the sampling time density before and after the

450   stage of interest. In addition, differences in individual development, such as different

451   growth rates, may also cause bias in the monthly differential expression analysis.

Abbreviations

453   SCG: Seasonal changing gene; CAM: Cell adhesion molecule; DEG: Differentially

454   expressed gene; Monthly DEG: Monthly differentially expressed gene; ECM:

455   Extracellular matrix; HF: Hair follicle; SHF: Secondary hair follicle; BMP: Bone

456   morphogenetic protein; SHH: Sonic hedgehog; FGF: Fibroblast growth factor; TGF:

457   Transforming growth factor; KRT: Keratin; KRTAP: Keratin-associated protein;

458   lncRNA: Long noncoding RNA; miRNA: MicroRNA; WGCNA: Weighted gene co-

459   expression network analysis; KEGG: Kyoto Encyclopedia of Genes and Genomes; GO:

460   Gene Ontology; BP: Biological process; PCA: Principal components analysis; LEF:

461   Lymphoid enhancer binding factor; IL: Interleukin; DKK: Dickkopf

Declarations

Ethics approval and consent to participate

464   The skin samples in this study were collected from the Inner Mongolia Cashmere Goats.

465   All procedures were conducted according to the standards of the Animal Care and Use

466   Committee in Inner Mongolia University for Nationalities, China.

Consent for publication

468   Not applicable.

Availability of data and materials

470   The authors acknowledge that the data presented in this study must be deposited and

471   made publicly available in an acceptable repository, prior to publication.

Competing interests

473   The authors declare that they have no competing interests.

Funding

481 study and data collection.

Authors' contributions

483 Chun Li conducted the research, Cong Feng and Guangyuan Ma analysed the data and

484 prepare the manuscript, Shaoyin Fu helped RNA-seq and data processing, Jinquan Li

485 and Wenguang Zhang provided the test platform, Ming Chen supervised data analysis

486 and manuscript revising.

Acknowledgments

488 The authors are thankful for the samples provided by the Hanshan White Cashmere

489 Goat Breeding Farm.

Author details

491 [1]College of Animal Science and Technology, Inner Mongolia University for

492 Nationalities, Tongliao 028000, China. [2]College of Life Sciences, Zhejiang University,

493 Hangzhou 310058, China. [3]Inner Mongolia Academy of Agricultural & Animal

494 Husbandry Sciences, Hohhot 010018, China. [4]College of Life Science and Food

495 Engineering, Inner Mongolia University for Nationalities, Tongliao 028000, China.

496 [5]College of Animal Science, Inner Mongolia Agricultural University, Hohhot 010018,

497 China.

498

499

500

501

502

References

504   1.   Zhu B, Xu T, Yuan J, Guo X, Liu D. Transcriptome Sequencing Reveals

505   Differences between Primary and Secondary Hair Follicle-derived Dermal Papilla Cells

506   of the Cashmere Goat (*Capra hircus*). PLoS One. 2013;8(9):e76282.

507   2.   Bykov YS, Schaffer M, Dodonova SO, Albert S, Plitzko JM, Baumeister W, et al.

508   The structure of the COPI coat determined within the cell. eLife. 2017;6.

509   3.   Pin D, Cachon T, Carozzo C. Determination of the Depth of Excision Using a

510   Dermatome (Aesculap®) to Export all Hair Follicle Bulbs from a Donor Site in the Dog.

511   J Vet Med A. 2007;54(9):539-41.

512   4.   McCarthy B. Specialty animal fibers. Textiles. 1998;20(1):6-8.

513   5.   Yang F, Liu Z, Zhao M, Mu Q, Che T, Xie Y, et al. Skin transcriptome reveals the

514   periodic changes in genes underlying cashmere (ground hair) follicle transition in

515   cashmere goats. BMC Genomics. 2020;21(1).

516   6.   Klören WRL, Norton BW. Melatonin and fleece growth in Australian cashmere

517   goats. Small Rumin Res. 1995;17(2):179-85.

518   7.   Betteridge K, Welch R, Pomroy W, Lapwood K, Devantier B, editors. Out of

519   season cashmere growth in feral goats. Proceedings of the second international

520   cashmere conference; 1987.

521   8.   Litherland AJ, Paterson DJ, Parry AL, Dick HB, Staples LD. Melatonin for

522   cashmere production. Proceedings of the New Zealand Society of Animal Production.

523   1990;50:339-43.

524   9.   Welch RAS, Gurnsey MP, Betteridge K, Mitchell RJ. Goat fibre response to

525 melatonin given in spring in two consecutive years. Proceedings of the New Zealand

526 Society of Animal Production. 1990;50:335-8.

527 10. Yang CH, Duan CH, Wu ZY, Li Y, Luan YY, Fu XJ, et al. Effects of melatonin

528 administration to cashmere goats on cashmere production and hair follicle

529 characteristics in two consecutive cashmere growth cycles. Domest Anim Endocrinol.

530 2021;74:106534.

531 11. Duan CH, Xu JH, Sun CM, Jia ZH, Zhang W. Effects of melatonin implantation

532 on cashmere yield, fibre characteristics, duration of cashmere growth as well as growth

533 and reproductive performance of Inner Mongolian cashmere goats. J Anim Sci

534 Biotechnol. 2015;6.

535 12. Tsai S-Y, Sennett R, Rezza A, Clavel C, Grisanti L, Zemla R, et al. Wnt/β-catenin

536 signaling in dermal condensates is required for hair follicle formation. Dev Biol.

537 2014;385(2):179-88.

538 13. Enshell-Seijffers D, Lindon C, Kashiwagi M, Morgan BA. β-catenin Activity in

539 the Dermal Papilla Regulates Morphogenesis and Regeneration of Hair. Dev Cell.

540 2010;18(4):633-42.

541 14. Veltri A, Lang C, Lien W-H. Concise Review: Wnt Signaling Pathways in Skin

542 Development and Epidermal Stem Cells. Stem Cells. 2018;36(1):22-35.

543 15. Yuhki M. BMPR1A signaling is necessary for hair follicle cycling and hair shaft

544 differentiation in mice. Development. 2004;131(8):1825-33.

545 16. Kulessa H. Inhibition of Bmp signaling affects growth and differentiation in the

546 anagen hair follicle. EMBO J. 2000;19(24):6664-74.

547   17. Woo WM, Zhen HH, Oro AE. Shh maintains dermal papilla identity and hair

548   morphogenesis via a Noggin-Shh regulatory loop. Genes Dev. 2012;26(11):1235-46.

549   18. Żak M, Klis SFL, Grolman W. The Wnt and Notch signalling pathways in the

550   developing cochlea: Formation of hair cells and induction of regenerative potential. Int

551   J Dev Neurosci. 2015;47(Part_B):247-58.

552   19. Rosenquist TA, Martin GR. Fibroblast growth factor signalling in the hair growth

553   cycle: Expression of the fibroblast growth factor receptor and ligand genes in the

554   murine hair follicle. Dev Dyn. 1996;205(4):379-86.

555   20. Choi YM, Choi SY, Kim H, Kim J, Ki MS, An I-S, et al. TGFβ family mimetic

556   peptide promotes proliferation of human hair follicle dermal papilla cells and hair

557   growth in C57BL/6 mice. Biomedical Dermatology. 2018;2(1).

558   21. Wang J, Sui J, Mao C, Li X, Chen X, Liang C, et al. Identification of Key Pathways

559   and Genes Related to the Development of Hair Follicle Cycle in Cashmere Goats.

560   Genes. 2021;12(2):180.

561   22. Nie Y, Li S, Zheng X, Chen W, Li X, Liu Z, et al. Transcriptome Reveals Long

562   Non-coding RNAs and mRNAs Involved in Primary Wool Follicle Induction in Carpet

563   Sheep Fetal Skin. Front Physiol. 2018;9.

564   23. Yin R, Wang Y, Zhao S, Yin R, Bai M, Wang Z, et al. LncRNA-599554 sponges

565   miR-15a-5p to contribute inductive ability of dermal papilla cells through positively

566   regulating the expression of Wnt3a in cashmere goat. Electron J Biotechnol. 2020;45.

567   24. Wang S, Ge W, Luo Z, Guo Y, Jiao B, Qu L, et al. Integrated analysis of coding

568   genes and non-coding RNAs during hair follicle cycle of cashmere goat (*Capra hircus*).

569   BMC Genomics. 2017;18(1).

570   25. Wang J, Che L, Hickford J, Zhou H, Hao Z, Luo Y, et al. Identification of the

571   Caprine Keratin-Associated Protein 20-2 (KAP20-2) Gene and Its Effect on Cashmere

572   Traits. Genes. 2017;8(11):328.

573   26. Sulayman A, Tian K, Huang X, Tian Y, Xu X, Fu X, et al. Genome-wide

574   identification and characterization of long non-coding RNAs expressed during sheep

575   fetal and postnatal hair follicle development. Sci Rep. 2019;9(1).

576   27. Andrews S. FastQC: a quality control tool for high throughput sequence data. 2010.

577   28. Pertea M, Kim D, Pertea GM, Leek JT, Salzberg SL. Transcript-level expression

578   analysis of RNA-seq experiments with HISAT, StringTie and Ballgown. Nat Protoc.

579   2016;11(9):1650.

580   29. Kang Y-J, Yang D-C, Kong L, Hou M, Meng Y-Q, Wei L, et al. CPC2: a fast and

581   accurate coding potential calculator based on sequence intrinsic features. Nucleic Acids

582   Res. 2017;45(W1):W12-W6.

583   30. Sun L, Luo H, Bu D, Zhao G, Yu K, Zhang C, et al. Utilizing sequence intrinsic

584   composition to classify protein-coding and long non-coding transcripts. Nucleic Acids

585   Res. 2013;41(17):e166.

586   31. Anders S, Pyl PT, Huber W. HTSeq—a Python framework to work with high-

587   throughput sequencing data. Bioinformatics. 2015;31(2):166-9.

588   32. Love MI, Huber W, Anders S. Moderated estimation of fold change and dispersion

589   for RNA-seq data with DESeq2. Genome Biol. 2014;15(12):1-21.

590   33. Langfelder P, Horvath S. WGCNA: an R package for weighted correlation network

591   analysis. BMC Bioinformatics. 2008;9(1):1-13.

592   34. Huang DW, Sherman BT, Tan Q, Kir J, Liu D, Bryant D, et al. DAVID

593   Bioinformatics Resources: expanded annotation database and novel algorithms to better

594   extract biology from large gene lists. Nucleic Acids Res. 2007;35(Web Server

595   issue):W169-W75.

596   35. Kanehisa M, Goto S. KEGG: kyoto encyclopedia of genes and genomes. Nucleic

597   Acids Res. 2000;28(1):27-30.

598   36. Ashburner M, Ball CA, Blake JA, Botstein D, Butler H, Cherry JM, et al. Gene

599   Ontology: Tool for the unification of biology. Nat Genet. 2000;25(1):25-9.

600   37. Yu G, Wang L-G, Han Y, He Q-Y. ClusterProfiler: an R Package for Comparing

601   Biological Themes Among Gene Clusters. OMICS: J Integrative Biol. 2012;16(5):284-

602   7.

603   38. Morgan M, Shepherd L. AnnotationHub: Client to access AnnotationHub

604   resources. https://bioconductor.org/packages/AnnotationHub/2020 [

605   39. Shannon P, Markiel A, Ozier O, Baliga NS, Wang JT, Ramage D, et al. Cytoscape:

606   a software environment for integrated models of biomolecular interaction networks.

607   Genome Res. 2003;13(11):2498-504.

608   40. Oshimori N, Fuchs E. Paracrine TGF-beta signaling counterbalances BMP-

609   mediated repression in hair follicle stem cell activation. Cell Stem Cell. 2012;10(1):63-

610   75.

611   41. Rishikaysh P, Dev K, Diaz D, Qureshi WM, Filip S, Mokry J. Signaling involved

612   in hair follicle morphogenesis and development. Int J Mol Sci. 2014;15(1):1647-70.

613   42. Zhang Y, Yu J, Shi C, Huang Y, Wang Y, Yang T, et al. Lef1 contributes to the

614   differentiation of bulge stem cells by nuclear translocation and cross-talk with the

615   Notch signaling pathway. Int J Med Sci. 2013;10(6):738-46.

616   43. Attisano L, Wrana JL. Signal integration in TGF-beta, WNT, and Hippo pathways.

617   F1000Prime Rep. 2013;5:17.

618   44. Hwang J, Mehrani T, Millar SE, Morasso MI. Dlx3 is a crucial regulator of hair

619   follicle differentiation and cycling. Development. 2008;135(18):3149-59.

620   45. Guo T, Han J, Yuan C, Liu J, Niu C, Lu Z, et al. Comparative proteomics reveals

621   genetic mechanisms underlying secondary hair follicle development in fine wool sheep

622   during the fetal stage. J Proteomics. 2020;223:103827.

623   46. St-Jacques B, Dassule H, Karavanova I, Botchkarev V, Li J, Danielian P, et al.

624   Sonic hedgehog signaling is essential for hair development. Curr Biol.

625   1998;8(19):1058-69.

626   47. Nanba D, Nakanishi Y, Hieda Y. Role of Sonic hedgehog signaling in epithelial

627   and mesenchymal development of hair follicles in an organ culture of embryonic mouse

628   skin. Dev Growth Differ. 2003;45(3):231-9.

629   48. Abe Y, Tanaka N. Roles of the Hedgehog Signaling Pathway in Epidermal and

630   Hair Follicle Development, Homeostasis, and Cancer. J Dev Biol. 2017;5(4).

631   49. Zhu B, Xu T, Zhang Z, Ta N, Gao X, Hui L, et al. Transcriptome sequencing

632   reveals differences between anagen and telogen secondary hair follicle-derived dermal

633   papilla cells of the Cashmere goat (*Capra hircus*). Physiol Genomics. 2014;46(3):104-

634   11.

635   50. Mueller SN, Germain RN. Stromal cell contributions to the homeostasis and

636   functionality of the immune system. Nat Rev Immunol. 2009;9(9):618-29.

637   51. Nagao K, Kobayashi T, Moro K, Ohyama M, Adachi T, Kitashima DY, et al.

638   Stress-induced production of chemokines by hair follicles regulates the trafficking of

639   dendritic cells in skin. Nat Immunol. 2012;13(8):744-52.

640   52. Scharschmidt TC, Vasquez KS, Pauli ML, Leitner EG, Chu K, Truong HA, et al.

641   Commensal Microbes and Hair Follicle Morphogenesis Coordinately Drive Treg

642   Migration into Neonatal Skin. Cell Host Microbe. 2017;21(4):467-77 e5.

643   53. Harel S, Higgins CA, Cerise JE, Dai Z, Chen JC, Clynes R, et al. Pharmacologic

644   inhibition of JAK-STAT signaling promotes hair growth. Sci Adv. 2015;1(9):e1500973.

645   54. Wang ECE, Dai Z, Ferrante AW, Drake CG, Christiano AM. A Subset of TREM2($^+$)

646   Dermal Macrophages Secretes Oncostatin M to Maintain Hair Follicle Stem Cell

647   Quiescence and Inhibit Hair Growth. Cell Stem Cell. 2019;24(4):654-69 e6.

648   55. Kim JE, Lee YJ, Park HR, Lee DG, Jeong KH, Kang H. The Effect of JAK

649   Inhibitor on the Survival, Anagen Re-Entry, and Hair Follicle Immune Privilege

650   Restoration in Human Dermal Papilla Cells. Int J Mol Sci. 2020;21(14).

651   56. Kwack MH, Kim MK, Kim JC, Sung YK. Dickkopf 1 promotes regression of hair

652   follicles. J Invest Dermatol. 2012;132(6):1554-60.

653   57. Kwack MH, Lee JH, Seo CH, Kim JC, Kim MK, Sung YK. Dickkopf-1 is involved

654   in dexamethasone-mediated hair follicle regression. Exp Dermatol. 2017;26(10):952-4.

655   58. Grosbois J, Demeestere I. Dynamics of PI3K and Hippo signaling pathways during

656   in vitro human follicle activation. Hum Reprod. 2018;33(9):1705-14.

657   59. Chen Y, Fan Z, Wang X, Mo M, Zeng SB, Xu RH, et al. PI3K/Akt signaling

658   pathway is essential for de novo hair follicle regeneration. Stem Cell Res Ther.

659   2020;11(1):144.

660   60. Nelson AM, Reddy SK, Ratliff TS, Hossain MZ, Katseff AS, Zhu AS, et al. dsRNA

661   Released by Tissue Damage Activates TLR3 to Drive Skin Regeneration. Cell Stem

662   Cell. 2015;17(2):139-51.

663   61. Wang X, Wang J, Guo L, Wang X, Chen H, Wang X, et al. Self-assembling peptide

664   hydrogel scaffolds support stem cell-based hair follicle regeneration. Nanomedicine.

665   2016;12(7):2115-25.

666   62. Millar SE, Willert K, Salinas PC, Roelink H, Nusse R, Sussman DJ, et al. WNT

667   Signaling in the Control of Hair Growth and Structure. Dev Biol. 1999;207(1):133-49.

668   63. Stenn KS, Paus R. Controls of Hair Follicle Cycling. Physiol Rev. 2001;81(1):449-

669   94.

670   64. Li Y-H, Zhang K, Yang K, Ye J-X, Xing Y-Z, Guo H-Y, et al. Adenovirus-

671   Mediated Wnt10b Overexpression Induces Hair Follicle Regeneration. J Invest

672   Dermatol. 2013;133(1):42-8.

673   65. Mill P. Sonic hedgehog-dependent activation of Gli2 is essential for embryonic

674   hair follicle development. Genes Dev. 2003;17(2):282-94.

675   66. Potter CS, Pruett ND, Kern MJ, Baybo MA, Godwin AR, Potter KA, et al. The

676   Nude Mutant Gene Foxn1 Is a HOXC13 Regulatory Target during Hair Follicle and

677   Nail Differentiation. J Invest Dermatol. 2011;131(4):828-37.

678   67. Yu X, Chen F, Ni C, Zhang G, Zheng L, Zhang J, et al. A Missense Mutation within

679   the Helix Termination Motif of KRT25 Causes Autosomal Dominant Woolly

680   Hair/Hypotrichosis. J Invest Dermatol. 2018;138(1):230-3.

681   68. Fujimoto A, Farooq M, Fujikawa H, Inoue A, Ohyama M, Ehama R, et al. A

682   Missense Mutation within the Helix Initiation Motif of the Keratin K71 Gene Underlies

683   Autosomal Dominant Woolly Hair/Hypotrichosis. J Invest Dermatol.

684   2012;132(10):2342-9.

685   69. Xu T, Guo X, Wang H, Hao F, Du X, Gao X, et al. Differential gene expression

686   analysis between anagen and telogen of *Capra hircus* skin based on the de novo

687   assembled transcriptome sequence. Gene. 2013;520(1):30-8.

688   70. Jin M, Cao M, Cao Q, Piao J, Zhao F, Piao Ja. Long noncoding RNA and gene

689   expression analysis of melatonin-exposed Liaoning cashmere goat fibroblasts

690   indicating cashmere growth. The Science of Nature. 2018;105(9):60.

691   71. Geng RQ, Yuan C, Chen YL. Exploring Differentially Expressed Genes by RNA-

692   Seq in Cashmere Goat (*Capra hircus*) Skin during Hair Follicle Development and

693   Cycling. PLoS One. 2013;8(4).

694   72. Su R, Fan YX, Qiao X, Li XK, Zhang L, Li C, et al. Transcriptomic analysis reveals

695   critical genes for the hair follicle of Inner Mongolia cashmere goat from catagen to

696   telogen. PLoS One. 2018;13(10).

697

698

699

700

701 **Figures**

702 **Figure 1. Overview of the transcriptome analysis.** (**A**) The control and melatonin

703 groups and sampling time. (**B**) Seasonal changing genes (SCGs) in the D and M groups.

704 (**C**) The number of coding genes, novel lncRNAs and annotated lncRNAs in the D and

705 M groups. The Venn plot indicates that 759 genes are detected in both D and M groups.

706 (**D**) PCA plot of the median-normalized samples in the D group. The circle suggests

707 the direction of samples in cashmere growth stages. (**E**) PCA plot of the median-

708 normalized samples in the M group. (**F**) The cashmere length change plot in the D group.

709 The shedding occurs in May-June. (**G**) The cashmere length change plot in the M group.

710 The first shedding occurs in May-June. Another shedding appears in September-

711 November.

712

713 **Figure 2. Stage-specific gene expression patterns and pathway enrichment.** (**A**)

714 Heatmap of the expression level of three D clusters (DC1, DC2 and DC3) in D and M

715 groups. (**B**) The number of coding genes, annotated lncRNAs and novel lncRNAs in

716 three D clusters. (**C**) KEGG pathway enrichment of the genes in DC1, DC2 and DC3.

717 The pathways shared by DC2 and DC3 are shown in black. (**D**) The expression trends

718 of three gene clusters. The cashmere growth cycle is divided into three stages according

719 to the expression patterns.

720

721 **Figure 3. Pathway-mRNA-lncRNA co-expression network.** A total of 16 signaling

722 pathways, 143 pathway genes, and 93 co-expressed lncRNAs (Pearson correlation ≥0.8)

723   are involved in this network. The size of the pathway node is positively related to its

724   degree.

725

726   **Figure 4. Analysis of differences in the expression patterns triggered by melatonin.**

727   (**A**) Venn diagrams showing SCGs in D clusters and M group and DCGs between D

728   and M groups. (**B**) The changed and unchanged genes of three D clusters after

729   melatonin treatment. (**C**) Heatmap of the expression level of three M clusters (MC1,

730   MC2 and MC3) in D and M groups. (**D**) The expression patterns of three M clusters in

731   D and M groups. (**E**) KEGG pathway enrichment of the genes in MC1, MC2 and MC3.

732

733   **Figure 5. Detection of monthly differential expressed genes (DEGs) triggered by**

734   **melatonin and pathway enrichment analysis.** (**A**) The number and distribution of

735   monthly differential expressed genes triggered by melatonin between M and D group.

736   (**B**) The KEGG pathway enrichment analysis of monthly differential expressed genes.

737   (**C**) The GO biological process enrichment analysis of monthly differential expressed

738   genes. Note that up-regulated and down-regulated genes in different months are

739   separated for GO & KEGG analysis, in which 'Up' represents up-regulated genes, and

740   'Down' represents down-regulated genes. The color of nodes represents adjusted p-

741   value, and the size of nodes represents the ratio of gene numbers.

742

743   **Figure 6. The putative pathway regulation model of the cashmere growth cycle**

744   **triggered by melatonin.** The signal pathways related to cashmere shedding are marked

745   with dotted line boxes, and the other solid line boxes mark the signal pathways which

746   may promote the hair follicle development.

747

748   **Tables**

749   **Table 1. Summary of representative GO & KEGG enrichment of monthly DEGs**

Cluster	Description	p.adjust	Gene Name
Month4_Up	hair cycle	0.0276	PTCH2, FOXE1, HOXC13, FOXN1
Month5_Up	hair cycle	0.0082	PTCH2, FOXE1, FOXN1, HOXC13, KRT71, KRT25
Month4_Up	Hedgehog signaling pathway	0.0306	SHH, PTCH2, PTCH1
Month4_Up	Wnt signaling pathway	0.0428	FZD10, WIF1, LEF1, WNT11
Month6_Down	ECM-receptor interaction	0.0259	COL6A3, THBS3, FREM1, COL1A1
Month7_Down	ECM-receptor interaction	0.0218	FREM1, FRAS1, FREM2
Month8_Down	Wnt signaling pathway	0.0257	WNT6, NOTUM, SFRP2
Month8_Down	Hedgehog signaling pathway	0.0318	SHH, PTCH2
Month9_Up	Chemokine signaling pathway	0.0002	CCL17, CCL22, CCL2, LYN, RAC2, LOC102170772, PIK3CG, VAV1
Month9_Up	NF-κB signaling pathway	0.0020	CD40LG, LTB, ZAP70, LYN, BTK

750   **Note**: The first two lines are derived from GO BP results and others are derived from

751   KEGG results. P.adjust represents adjusted p-values.

752

753

754

755

Additional files

756 **Additional files**

757 **Additional file 1: Table S1.** Read counts of all detected genes in 72 samples.

758 **Additional file 2: Table S2.** Predicted lncRNAs.

759 **Additional file 3: Table S3.** Differentially expressed genes in the control group.

760 **Additional file 4: Table S4.** Differentially expressed genes in the melatonin-treated

761 group.

762 **Additional file 5: Table S5.** Detailed genes of 3 clusters in the control group (DC1,

763 DC2 and DC3).

764 **Additional file 6: Table S6.** The KEGG enrichment results of genes in DC1, DC2 and

765 DC3.

766 **Additional file 7: Table S7.** The Pearson correlations between genes and lncRNAs.

767 **Additional file 8: Table S8.** Genes with different expression patterns between the

768 control and melatonin-treated groups.

769 **Additional file 9: Table S9.** Detailed genes of 3 clusters in the melatonin-treated group

770 (MC1, MC2 and MC3).

771 **Additional file 10: Table S10.** The KEGG enrichment results of genes in MC1, MC2

772 and MC3.

773 **Additional file 11: Table S11.** The KEGG analysis results of monthly DEGs.

774 **Additional file 12: Table S12.** The GO analysis results of monthly DEGs.

775 **Additional file 13: Figure S1.** Boxplots of relative expression levels of HOXC13(A),

776 KRT25(B), FOXN1(c), KRT71(D). **Figure S2.** Boxplots of relative expression levels

777 in WNT signaling pathway (Wif-1(A), WNT11(B), FZD10(C), LEF1(D), NOTUM(E),

778   SFRP2(F), WNT6(G)). **Figure S3.** Boxplots of relative expression levels in Hedgehog

779   signaling pathway (Shh(A), PTCH1(B), PTCH2(C), FOXE1(D)). **Figure S4.** Boxplots

780   of relative expression levels of ECM related genes (FREM1(A), FREM2(B),

781   FRAS1(C), COL1A1(D), COL6A3(E), THBS3(F)). **Figure S5.** Boxplots of relative

782   expression levels of Chemokine related genes (CCL22(A), LYN(B), PIK3CG(C),

783   VAV1(D), RAC2(E), CCL17(F), CCL2(G), LOC102170772(H)). **Figure S6.** Boxplots

784   of relative expression levels in NF-κB signaling pathway (ZAP70(A), LYN(B),

785   BTK(C), CD40LG(D), LTB(E)).

786   **Additional file 14: Figure S1.** Chemokine Signaling Pathway virtualized by KEGG

787   Pathway Maps. **Figure S2.** ECM-Receptor Interaction Signaling Pathway virtualized

788   by KEGG Pathway Maps. **Figure S3.** NF-Kappa B Signaling Pathway virtualized by

789   KEGG Pathway Maps. **Figure S4.** Rap1 Signaling Pathway virtualized by KEGG

790   Pathway Maps. **Figure S5.** Hedgehog Signaling Pathway virtualized by KEGG

791   Pathway Maps. **Figure S6.** Wnt Signaling Pathway virtualized by KEGG Pathway

792   Maps. High-expressed monthly DEGs are highlighted with pink color, while low-

793   expressed monthly DEGs are highlighted with blue color.
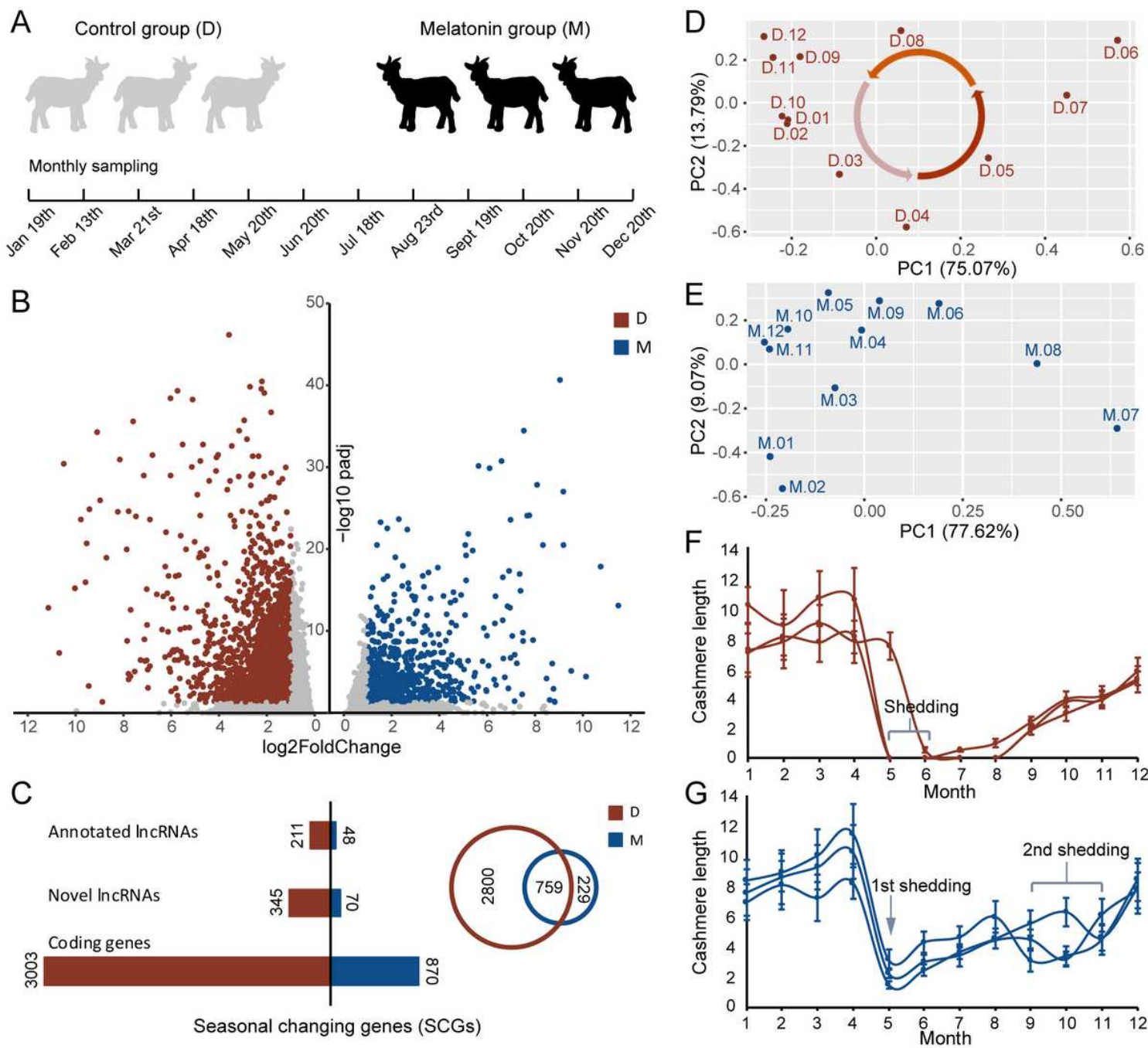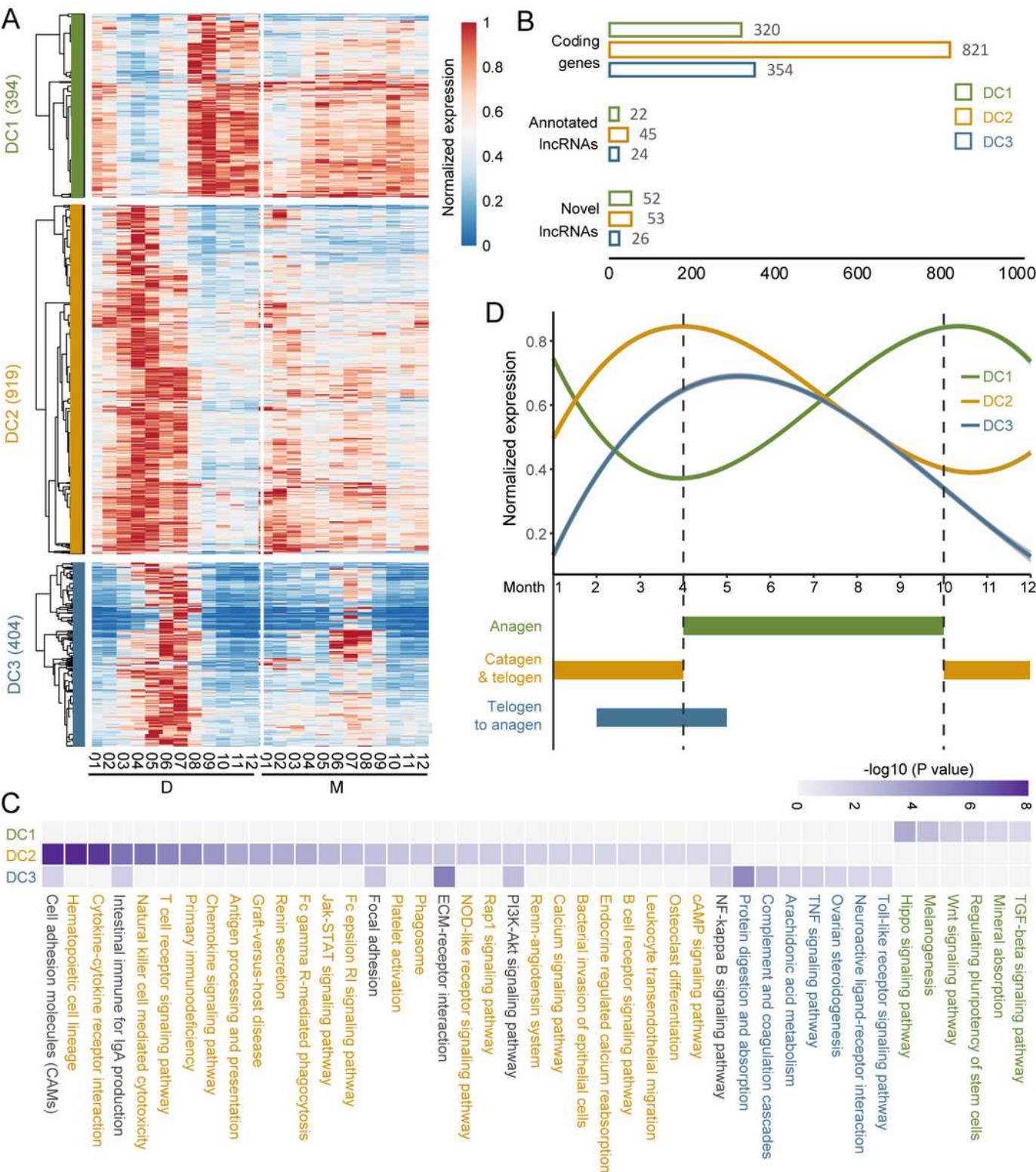
794

Figures

Figure 1

Overview of the transcriptome analysis. (A) The control and melatonin groups and sampling time. (B) Seasonal changing genes (SCGs) in the D and M groups. (C) The number of coding genes, novel lncRNAs and annotated lncRNAs in the D and M groups. The Venn plot indicates that 759 genes are detected in both D and M groups. (D) PCA plot of the median-normalized samples in the D group. The circle suggests the direction of samples in cashmere growth stages. (E) PCA plot of the median normalized samples in the M group. (F) The cashmere length change plot in the D group. The shedding occurs in May-June. (G)

The cashmere length change plot in the M group. The first shedding occurs in May-June. Another shedding appears in September- November.

Figure 2

Stage-specific gene expression patterns and pathway enrichment. (A) Heatmap of the expression level of three D clusters (DC1, DC2 and DC3) in D and M groups. (B) The number of coding genes, annotated lncRNAs and novel lncRNAs in three D clusters. (C) KEGG pathway enrichment of the genes in DC1, DC2

and DC3. The pathways shared by DC2 and DC3 are shown in black. (D) The expression trends of three gene clusters. The cashmere growth cycle is divided into three stages according to the expression patterns.

Figure 3

Pathway-mRNA-lncRNA co-expression network. A total of 16 signaling pathways, 143 pathway genes, and 93 co-expressed lncRNAs (Pearson correlation ≥0.8) are involved in this network. The size of the pathway node is positively related to its degree.
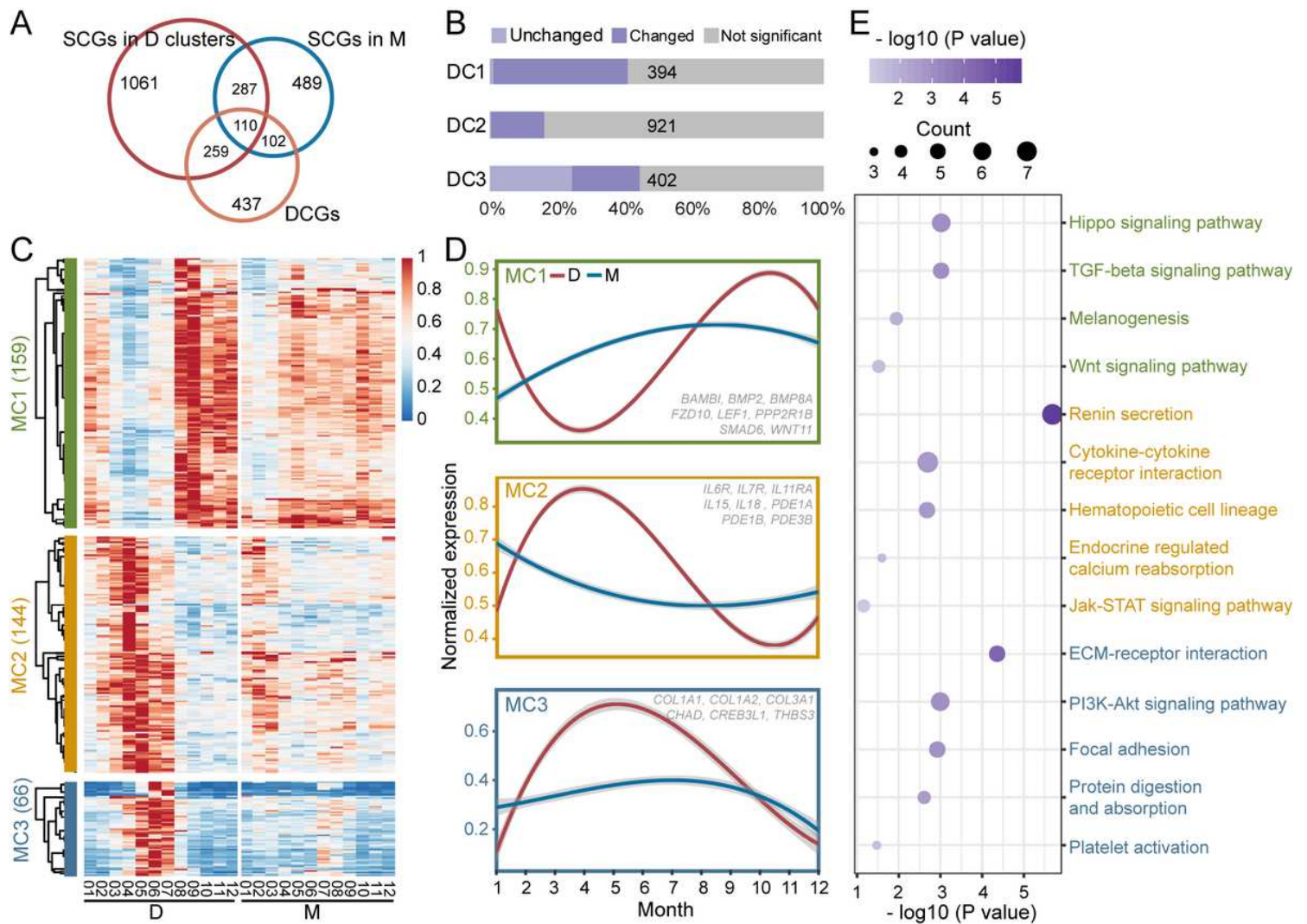
Figure 4

Analysis of differences in the expression patterns triggered by melatonin. (A) Venn diagrams showing SCGs in D clusters and M group and DCGs between D and M groups. (B) The changed and unchanged genes of three D clusters after melatonin treatment. (C) Heatmap of the expression level of three M clusters (MC1, MC2 and MC3) in D and M groups. (D) The expression patterns of three M clusters in D and M groups. (E) KEGG pathway enrichment of the genes in MC1, MC2 and MC3.
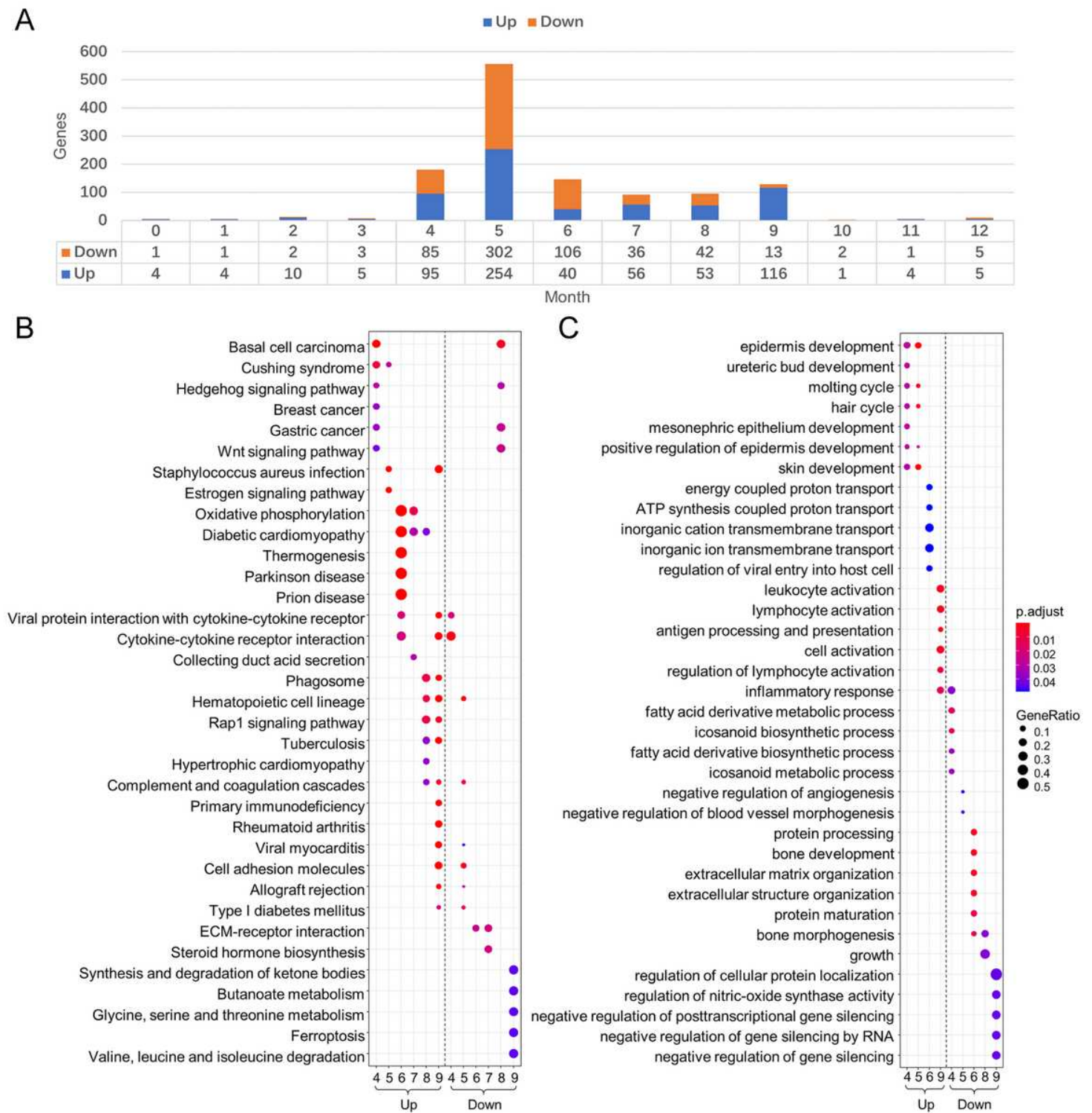
Figure 5

Detection of monthly differential expressed genes (DEGs) triggered by melatonin and pathway enrichment analysis. (A) The number and distribution of monthly differential expressed genes triggered by melatonin between M and D group. (B) The KEGG pathway enrichment analysis of monthly differential expressed genes. (C) The GO biological process enrichment analysis of monthly differential expressed genes. Note that up-regulated and down-regulated genes in different months are separated for GO & KEGG analysis, in which 'Up' represents up-regulated genes, and 'Down' represents down-regulated genes.

The color of nodes represents adjusted p value, and the size of nodes represents the ratio of gene numbers.
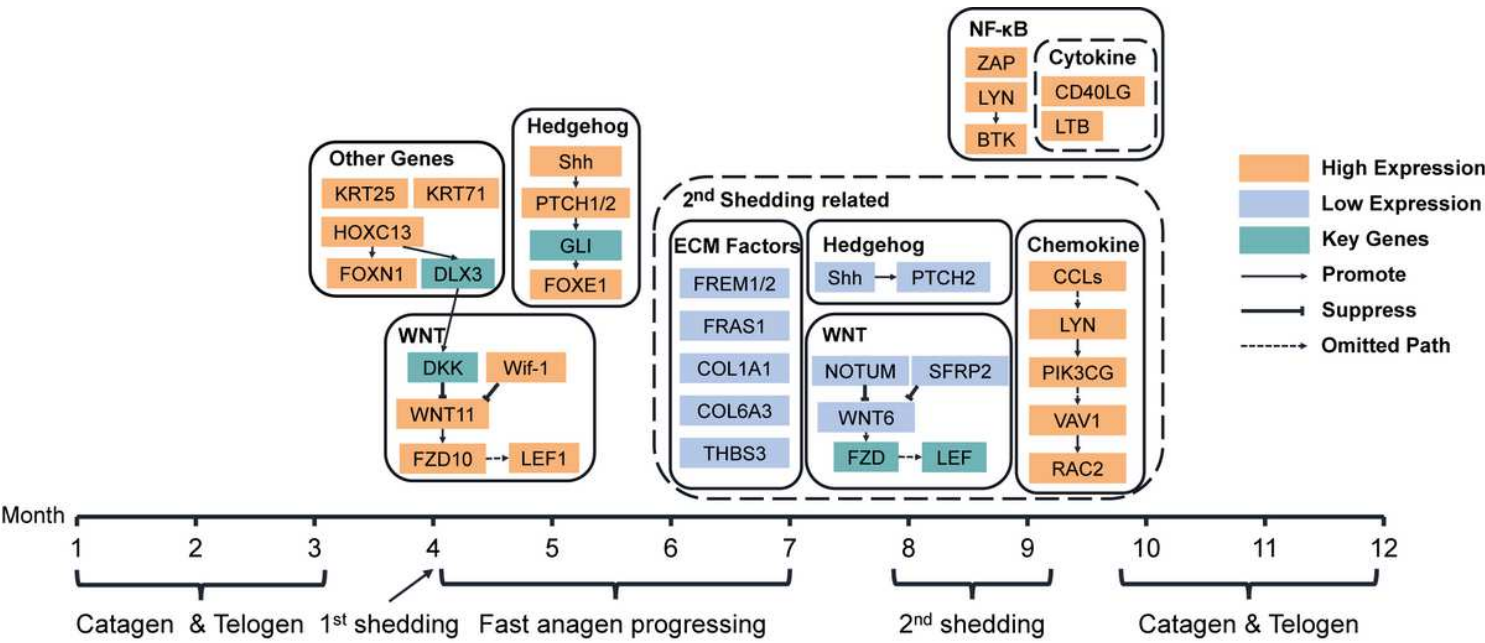

Figure 6

The putative pathway regulation model of the cashmere growth cycle triggered by melatonin. The signal pathways related to cashmere shedding are marked with dotted line boxes, and the other solid line boxes mark the signal pathways which may promote the hair follicle development.

Supplementary Files

This is a list of supplementary files associated with this preprint. Click to download.

- AdditionalFile1.csv
- AdditionalFile10.csv
- AdditionalFile11.csv
- AdditionalFile12.csv
- AdditionalFile13.docx
- AdditionalFile14.docx
- AdditionalFile2.csv
- AdditionalFile3.csv
- AdditionalFile4.csv
- AdditionalFile5.csv
- AdditionalFile6.csv
- AdditionalFile7.csv

- AdditionalFile8.csv
- AdditionalFile9.csv